

Influence of Firing Temperature on Compositional and Structural Properties of TiO₂ Thick Films

C.G. DIGHAVKAR¹*, A.V. PATIL¹, S.J. PATIL² and R.Y. BORSE²

¹Department of Electronic Science,

Loknete Vyankatrao Hiray Mahavidyalaya, Panchvati, Nasik

²Thin and Thick Film Laboratory, Department of Electronic Science, M.S.G. College,

Malegaon Camp, Maharashtra-423105, India

*E-mail:cgdighavkar@gmail.com

Abstract

TiO₂ thick films prepared by a standard screen printing method and fired between 600°C to 1000°C for 2-hours in an air atmosphere. Morphological, compositional, structural properties of the samples were analyzed by scanning electron microscopy (SEM), energy dispersive X-ray spectroscopy (EDS) and X-ray diffraction (XRD). X-ray diffraction shows that films are a mixture of anatase and rutile structures. During firing there was a phase transformation up to 900°C and at 1000°C the anatase phase disappeared and only rutile phase was found. Scanning electron microscopy shows that the grain size increases as the firing temperature increases. From X-ray diffraction using Scherrer's formula the crystallite size was measured. The crystallite size change from 12.08 to 36.42 nm was found to increase with the firing temperature.

Key words : TiO₂, screen printing, thick films, firing, crystallinity.

I. Introduction

In the wake of globalization in the twenty first century, there is tremendous advancement of science and technology. Due to this advancement, human life is becoming more and more comfortable. But this comfort of human being is at the cost of environmental pollution. To monitor this pollution, sensors with appropriate instrumentation are necessary. To have better performance, various sensors were developed. During the last decade and even now, the synthesis of novel materials for sensors and development of sensors continue to be the focus of active research in many areas of science and technology. The interdisciplinary nature of the sensor research brings scientists from various disciplines and the engineers together to work for the development of sensor systems. So, there is a great interest in implementing sensing devices in

order to improve environmental and safety control of gases. There is also a great need of this kind of sensors to carry out the optimization of combustion reactions in the emerging transport industry and in domestic and industrial applications. The gas sensors can be used as fire detectors, leakage detectors, controllers of ventilation in car and planes, alarm devices to indicate higher concentrations hazardous gases than its threshold values, detectors of volatile organic compounds and smells from food in the houses or in the food industries. Semiconductor oxide gas sensors are the best candidates to the development of commercial gas sensors for a wide range of such applications. The most used gas sensor devices can be divided into three big groups depending on the technology applied in their development: Solid state, Spectroscopic and Optic. While spectroscopic and optic sensors are very expensive for domestic use and sometimes difficult

to implement in reducing spaces. So-called Solid State sensors present great advantages due to their fast sensing response, simple implementation and low prices [1,2]. These Solid State gas sensors are based on the change of the physical and/or chemical properties of sensing materials when exposed to various gas atmospheres. Although the number of materials used to implement this kind of devices is huge, this work centered here in studying ones based semiconductor properties, and more specifically in using TiO₂ with various dopants as sensing materials. The development of TiO₂ thick films is of particular interest due to the numerous technological applications of this inorganic metal oxide. Metal oxide semiconducting materials like TiO₂, ZnO, SnO₂ and WO₃ appears the best candidates for gas sensing, as they operate reversibly and usually have stable chemical and thermal properties over extended periods of use [3]. TiO₂ thin and thick films are highly popular for such applications, where changes in the film electrical conductivity can be related to the physisorption and chemisorption of oxygen atoms [4, 5]. Titanium dioxide has many excellent physical properties such as a high dielectric constant, a strong mechanical and chemical stability, as well as good insulating properties. Due to its high refractive index and optical transmittance in the visible range, TiO₂ is especially suitable as material for optical coating and protective layers for very large-scale integrated circuits. Titanium dioxide (TiO₂) is extensively studied because of its broad range of applications in different fields. The increased interest in both the application and fundamental research of this material in the last decade is due to its remarkable optical and electrical properties. It is reported on its use as gas sensor, humidity and temperature sensor [6]. It is widely used in confectionery, cosmetics and food in plastic industry [7]. It is investigated as a key material for applications in photovoltaic cells, batteries, chemical sensing [8]. Thin and thick films of TiO₂ were made by sputtering and screen printing technique for NO₂ and CO gas sensors respectively [9]. Nano structured Nb-doped TiO₂ thick films have been prepared by screen printing process for CO gas sensors [10]. Also for same doping O₂

sensitivity has been reported [11]. TiO₂ is highly oxygen deficient so behaves as semiconducting oxide due to non-stoichiometry behavior. Recently buried contact solar cells have been fabricated using TiO₂ as an optical coating. It is used as piezoelectric crystal sensor for the detection of organic vapors using nanocrystalline [12]. It has interesting applications in chemistry due to its behavior as a reaction catalyst [13]. TiO₂ is used as photo catalytic degradation of phenol one of the most water pollutants [14] and environmental purification [15]. Titanium dioxide occurs in nature in three crystalline forms: Anatase, brookite and rutile. These crystals are essentially pure titanium dioxide but certain amount of impurities such as iron, chromium or vanadium darkens them. Rutile is thermodynamically stable form at all temperatures and is one of the important ores of titanium [16]. Several deposition techniques have been developed to grow undoped and doped TiO₂ films such as spray pyrolysis evaporation, chemical vapour deposition, sol gel technique, magnetron sputtering, pulsed laser deposition, spin coating and screen printing technique [17-23].

The aim of the present study is to prepare TiO₂ thick films by using a Standard Screen Printing Method on alumina substrates and study their structural, surface morphological and compositional properties at different firing temperature. Such a detailed understanding of the film properties are necessary if TiO₂ is to be developed to a degree which will enable its use in gas or humidity sensing devices. The aforementioned background justifies the need to improve the properties and features of these oxides in order to obtain a more efficient material for gas sensing purposes.

2. Experimental

Analar Reagent (AR) grade TiO₂ powder was calcined at 400 °C for 2 h in a muffle furnace. Then this powder was crushed and thoroughly mixed with a glass frit (PbO-70%, SiO₂-18%, Al₂O₃-9% and B₂O₃-3%) as a permanent binder. Organic vehicles such as butyl carbitol acetate (BCA) and ethyl cellulose (EC) were added to this mixture to achieve

proper thixotropic properties of the paste. The ratio of inorganic to organic parts was maintained at 70:30 (the ratio of active powder to permanent binder was kept at 95:5 in 70% and the ratio of EC to BCA was 98:2 in 30%). TiO₂ thick films were prepared on alumina substrates using a standard screen-printing technique. The screen of nylon (40s, mesh no.355) was selected for screen-printing. The required mask (2 × 1.25 cm) was developed on the screen using a standard photolithography process. The paste was printed on clean alumina substrates (5 × 2 cm) with the help of a mask. The pattern was allowed to settle for 15 to 20 minutes in air. The films were dried under infrared radiation for 45 minutes and fired at temperatures of 600, 700, 800, 900 and 1000 °C for 1.5 to 2 h (which includes the time required to achieve the peak firing temperature and then constant firing for 30 minutes at the peak temperature) in a muffle furnace. The structural properties of TiO₂ films were investigated using X-ray diffraction analysis from 20-80° [Rigaku diffractometer (Miniflex Model, Rigaku, Japan) with CuKα, λ=0.1542 nm radiation] with a 0.1°/step (2θ) at the rate of 2 s /step. A scanning electron microscopy (SEM- JOEL JED-2300) was employed to characterize the surface morphology. The composition of TiO₂ thick film samples were analyzed by an energy dispersive X-ray spectrometer (EDS) (JOEL-JED 6360 LA). The thickness of the TiO₂ thick films was measured using a Taylor-Hobson (Taly-step UK) system. The thickness of the films was observed to be uniform in the range of 15μm to 25μm.

The weight fraction of rutile (W_R) can be calculated from spurr formula.

$$W_R = I_R / (0.884 I_A + I_R) \quad (1)$$

where, I_A represents the integrated intensity of the anatase (101) peak, and I_R is the integrated intensity of rutile (110) peak.

The crystallite size was determined using Scherrer's formula.

$$D = \frac{0.9\lambda}{\beta \cos \theta} \quad (2)$$

where D is the crystallite size, λ is the wavelength of the X-ray radiation (1.542Å), β is the peak full width half maxima of the (101) peak of the XRD pattern and θ is the diffraction angle.

The information about the crystalline shape and sizes of TiO₂ thick film materials is obtained by using SEM [Model JEOL JED-2300(LA) Germany]. For SEM all the TiO₂ samples were coated with a very thin conducting gold layer (few100Å) using vacuum evaporation/sputtering technique to avoid charging of the samples. The composition of TiO₂ thick film samples was analyzed by Energy Dispersive Spectrometer (EDAX) (JEOL-JED 6360 LA).Brunauer-Emmett-Teller (BET) method was applied for specific surface area evaluation and was calculated for spherical particles using the following equation [29].

$$S_w = 6 / \rho d \quad (3)$$

where d is the diameter of the particles, ρ is the density of the particles.

3. Results and Discussion

3.1 Preheat Treatment

The preheat treatment for the material is necessary to decrease posterior materials instabilities. During this heat treatment the materials were submitted to high calcinations temperature to avoid instabilities during their working life. The calcinations of the powder before the paste preparation and the firing process of the printed film can determine the sensitivity of the active material layer. With calcinations, grain boundaries were developed and the powder sintered to bigger agglomerations. This causes development in higher surface area after firing and attains higher sensitivity to the layer [24].

A drying stage is required to remove the organic solvents, make the printed film adhere to the substrate and be relatively immune to smudging. After printing, the film was allowed to settle in air for a few minutes so that some of the volatile

solvents were evaporated slowly at room temperature. The organic agent was still present in the paste at this stage. Drying took place at temperatures between 70-180°C either in a conventional oven or by placing films under infrared radiation [24].

The high temperature firing cycle is designed to remove the remaining organic binders, to develop the structural and electrical properties of the film and to bond the film to the substrate. Temperatures up to 1000°C are required to achieve these objectives. During this firing process the glass frit melts and grains of the functional materials are held together and also the film becomes bonded firmly to the substrate. There are three distinct regions in this firing cycle. Firstly the temperature slowly was increased towards the peak firing temperature. During this time the remaining organics were removed. This occurred at 350-400°C. As the temperature reached 600-1000°C, the glass frit softens. Secondly the temperature remained constant for about 30 minutes. During this time the active material sintered and various reactions took place. The electrical properties of the film began to develop. Finally there was a cooling stage to room temperature that allows the glass frit to solidify [24]. Softening point of glass frit is in between the temperature range 500-700°C [25]. Hence the minimum and maximum firing temperature range was selected 600°C and 1000°C respectively. Films fired at 600°C and 700°C did not show better adhesiveness to substrate hence these films would not be suitable for gas/humidity sensing or further applications.

3.2 Elemental Analysis

Table I shows the composition of the films fired at different temperatures. The EDS spectrum showed the presence of only Ti and Oxygen. From the analysis it was found that the TiO₂ films are non-stoichiometric. The deficiency or excess of any type of atom in the crystal results in a distorted band

structure, with a corresponding increase in conductivity. Titanium oxide loses oxygen on heating so that Ti is then in excess. The oxygen, of course, evolves as an electrically neutral substance so that it is associated with each excess Ti ions in the crystal; there will be two electrons that remain trapped in the solid material, thus leading to non-stoichiometry in the solid. This leads to the formation of the n-type semiconductor [26, 27]. The EDS results show lot of variation Ti/O ratio with firing temperature.

Table I

Element (Mass %)	Composition of TiO ₂ obtained from EDS Firing Temperature		
	800°C	900°C	1000°C
Ti	60.27 %	57.63 %	59.92 %
O	39.73 %	42.37 %	40.08 %

The mass % of Ti and O in each sample was not as per the stoichiometric proportion and all samples were observed to be oxygen deficient. Excess or deficiency of the constituent material particles leads to the semiconducting nature of the material. It is found that high value of Ti/O ratio for TiO₂ film is at 800°C firing temperature. Therefore the TiO₂ thick film with optimized firing temperature of 800°C is chosen for further studies of pure TiO₂ samples.

3.3 Structural Parameters and Their Analysis

Figure 1 shows X-ray diffraction patterns obtained for TiO₂ thick films deposited on alumina substrates and fired at 600, 700, 800, 900 and 1000 °C. In all cases, the observed peaks A (101), A (200), A (211), A (204), A (301), P (110), R (101), R (210), and R (211) showed the presence of different phase of TiO₂, match well with reported JCPDS data 21-1272 and 21-1276 for anatase and rutile respectively confirming polycrystalline structure of the film. Alumina substrate (Al₂O₃) peaks are also appeared in XRD.

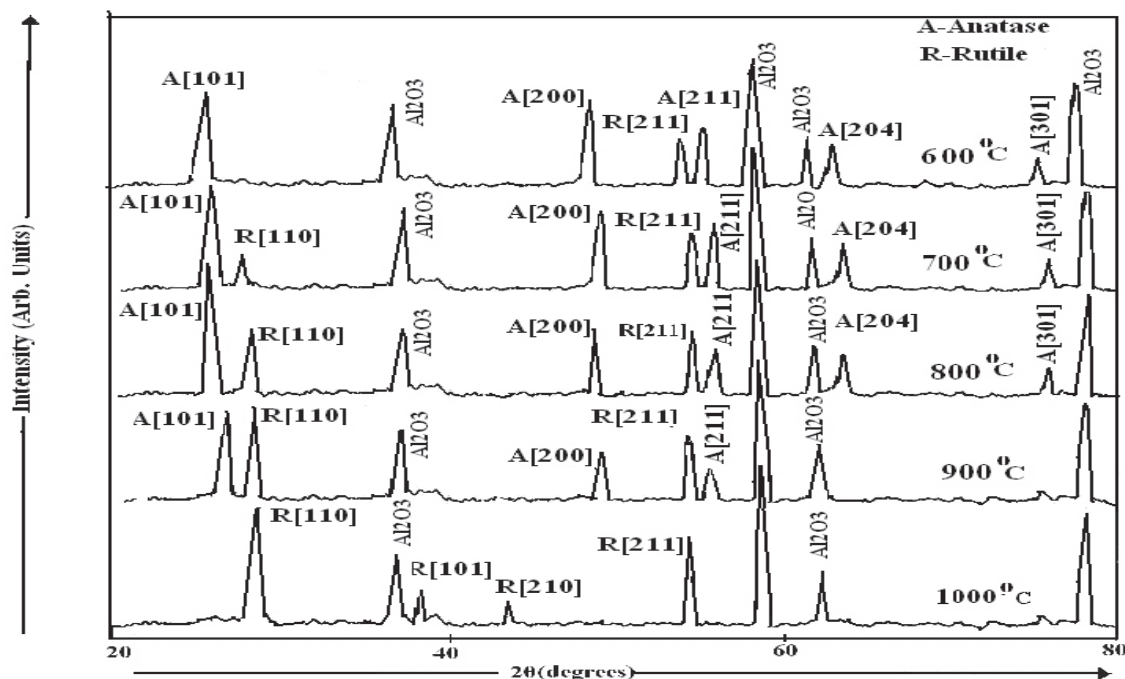


Fig. 1. XRD Pattern of TiO_2 films at different firing temperatures

It has been observed that the XRD peak broadening decreases with an increase of the firing temperature. The intensity of reflections increases with a rise in the firing temperature. Also XRD analysis evaluates the grain size of the thick films as function of the temperature. From this analysis all films were shown random orientation of polycrystalline nature of the material. The most pronounced and strongly reflected peak [101] of an anatase structure was observed at 25.8° and [110] of rutile structure at 28° for the temperature 800 and 1000°C respectively. The anatase phase transformation takes place up to 900°C , and at 1000°C no trace of anatase is observed in the XRD pattern. The intensity of anatase peak decreases as the firing temperature increases. This reduction of intensity indicates a decrease in the anatase content of the TiO_2 film [26]. Up to 900°C firing temperature both the phase of anatase and rutile were observed. The intensity of anatase phase decreased at 900°C firing temperature and disappeared completely at 1000°C . This clearly

indicates that phase transformation takes place up to 900°C and at firing temperature 1000°C only rutile phase was observed. The phase content of a sample can be calculated from the integrated intensities of the above-mentioned anatase and rutile peaks. If a sample contains mixture of anatase and rutile phase, the weight fraction of rutile (W_r) can be calculated from spurr formula equation-I [28, 29, 30 and 31]. The intensity of the rutile peak significantly increased while that of anatase peak decreased as shown in Table 2. The difference in the crystal structure in our titania powders with different anatase/rutile ratio is due to a thermal treatment at varying temperature of the anatase precipitate and spontaneous transformation from anatase to rutile. This transformation is an irreversible metastable to stable phase transition in temperature range $600\text{-}1000^\circ\text{C}$. Same trend was reported by S. Bakardjieva et al. at different temperature and pressure conditions [29].

Thick film fired at 800°C was shown good

Table 2
Weight % of anatase and rutile phase

Firing Temperature in °C	$I_A[101]$	$I_R[110]$	Anatase by XRD (W_A) in %	Rutile by XRD (W_R) in %
600	580	0	100	0
700	681	183	76.69	23.31
800	751	279	70.42	29.58
900	460	406	50.07	49.93
1000	0	468	0	100

adhesion to the alumina substrate and dominating phase of anatase. The electrical mobility of anatase films has much larger due to the smaller electron effective mass and also the Fermi level is higher about 0.1 eV compared to the rutile structure. So these properties are useful for gas sensing and other applications. In particular, anatase TiO₂ is extensively used in gas sensing [32, 33]. Also for further elevated temperature surface area decreases as grain size increases hence sensitivity decreases [33, 34]. In the field of chemical sensors, the structural stability, porosity and high surface to volume ratio are key

properties for a sensing film [35].

3.3.1 Crystallite size or grain size (D)

The XRD pattern was used to calculate the crystallite size of TiO₂ by using Eq. (2) (Scherrer's formula) [36]. The crystallite size of TiO₂ films at different firing temperatures is given in Table 3. The crystallite size of the film was found to be increase with an increase of the firing temperature as shown in Fig. 2.

3.4 Surface Morphology Analysis

Figure 3 (a), (b) and (c) represents the SEM

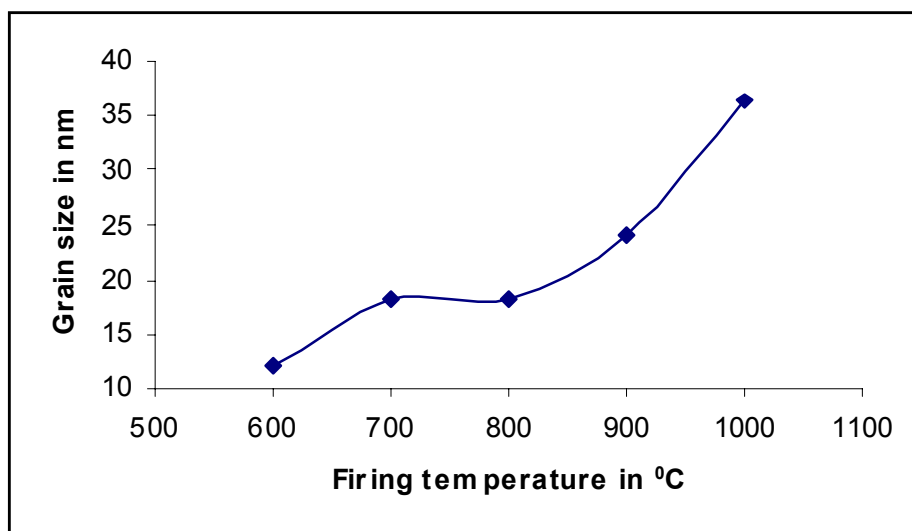


Fig. 2. Variation in crystallite size with temperature

images of TiO_2 Thick films fired at 800, 900 and 1000°C respectively. All the images are recorded at 10,000x magnification for the comparison. The SEM pictures clearly shown that the crystallite size increases with an increase in the firing temperature. Surface morphology has shown the particle sizes are the function of the temperature. The anatase consisting of spherical particles of 200 to 300 nm dimensions where as rutile appeared as elongated rods of 2.5 μm lengths. Microstructural parameters like crystallite size and RMS strain with the firing temperature clearly shows a marginal increase up to 900°C and beyond this temperature anatase phase disappear or transforms to rutile phase. The crystallite size of rutile phase increases rapidly at 1000°C resulting in growth of hexagonal shaped crystallite of phase oriented at (110) plane. From the micrograph analysis it is seen that at higher

temperatures polygonization of these dislocations with lowering of dislocation density at the grain boundary possibly favors the growth large sized crystallite of rutile phase [38, 39]. It has been observed that an increase in the firing temperature leads to an increase in the crystallite size and decrease in surface area. The loss in surface area available upon elevated heat treatment would affect the sensitivity [29, 37].

Defect disorder is very sensitive to oxygen activity, which imposed by the gas phase during processing of TiO_2 at elevated temperatures. The firing increases the atomic mobility; the atoms can be moved to more energetically favoured sites such as voids, grain boundaries and interstitial positions. An increase in temperature improves the crystallinity and thus increases the mobility of atoms

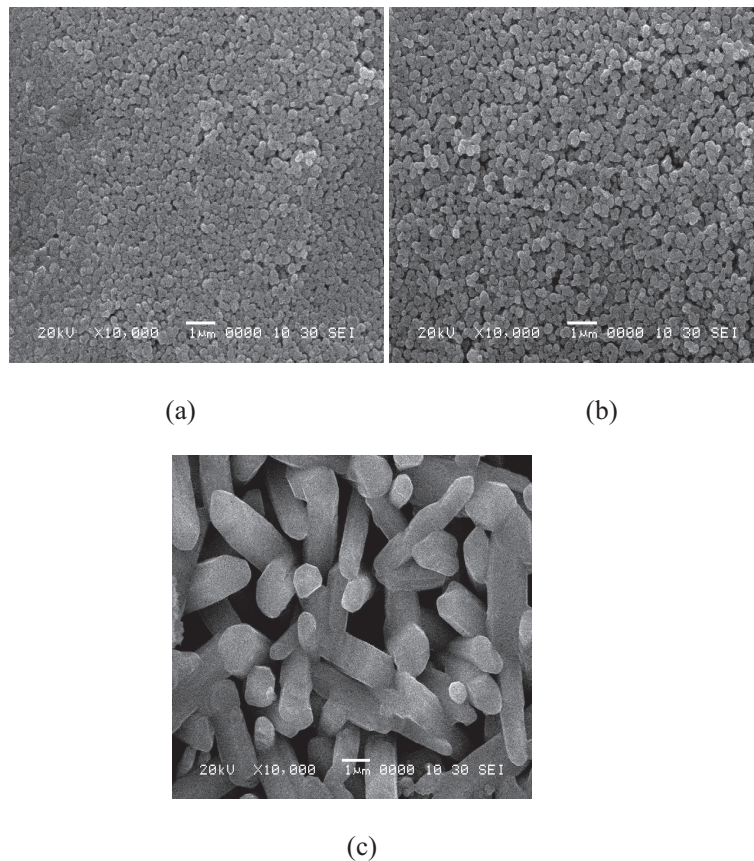


Fig.. 3. Scanning Electron Micrograms of TiO_2 thick film samples fired at (a) 800 (b) 900 and (c) 1000°C

Table 3
Microstructural Parameters of TiO₂ films fired at different temperatures

Firing Temp. in 0C	Crystallite (Grain)Size((D) In nm	Particle Size In nm	Surface Area(Sw) m ² /g
800	18.08	200	7.71
900	23.94	280	5.50
1000	36.42	1.7 μm	1.41

at the surface of the films [40].

Specific Surface Area (Sw)

The specific surface area increases as the size of the grains decreases. It was measured by the BET by using Eq. (3) [29]. The particle size increases with an increase in the firing temperature hence specific surface area decreases. Normally, the smaller its grain size, specific surface area and oxygen adsorption quantity, the higher its gas sensitivity. The sensing properties of materials always benefit from the large specific surface area, which can improve the interaction between oxygen and material surface [29]. The surface area of TiO₂ films at different firing temperatures is shown in Table 3.

4. Conclusion

TiO₂ thick films were prepared on alumina substrate by standard screen printing technique which is simple and an inexpensive method. From EDS and SEM it was confirmed that TiO₂ films were non-stoichiometric, which are suitable for gas sensing application. The films fired in the temperature range of 600-1000°C, were found polycrystalline. Films fired at 600°C and 700°C did not show better adhesiveness to substrate hence these films will not be suitable for gas/humidity sensing or further applications. Transformation of anatase phase to rutile phase was found up to 900°C. At 1000°C only rutile phase was found. The grain size increases with an increase in the firing temperature hence specific surface area decreases. Film fired at 800°C observed optimum surface area than further elevated temperatures. Film fired at 800°C was

shown more crystalline, porous, oxygen deficient, optimum specific surface area and good adhesion to alumina substrate. The film fired at this temperature may be suitable candidate for sensing applications. An increase in temperature improves the crystallinity and thus increases the mobility of atoms at the surface of the films.

Acknowledgement

The authors are thankful to Management authorities of M.G. Vidyamandir, Malegaon (Nasik), The Principal, M.S.G. College, Malegaon, The Principal L.V.H. College, Nasik.

References

- [1] H. Meixner, J. Gerblinger, U. Lampe and M. Fleisher, Thin-film gas sensors based on Semiconducting metal oxides, *Sensors and Actuators B*, **23** (1995) 119.
- [2] T. Takeuchi, Oxygen Sensors, *Sensors and Actuators B*, **14** (1988) 109.
- [3] M.Z. Atashbar, H.T. Sun, B. Gong, W. Wlodarski and R. Lamb, *Thin Solid Films*, **326** (1998) 238.
- [4] T. Takeuchi, *Sensor and Actuators B: Chemical*, **14** (1988) 109.
- [5] W. Gopel, G. Roker and R. Feierabend, *Phys. Rev. B*, **28** (1993) 3427.
- [6] S.R. Dhage, R. Pasricha and V. Ravi., *Mater. Res.*, **B 38** (2003) 1623.
- [7] C. Raymond, J. Paul, Y. Sheskey and Paul J. Weler, *Handbook of Pharmaceutical*

- Excipients (4th edition), Alpha-American Pharmaceutical Press, (2006) 6513.
- [8] O.K. Varghse, D.W. Gong, M. Paulose, K.G. Dong and C.A. Grimes, *Adv. Matr.*, **15** (2003) 15624.
- [9] V. Guidi, M.C. Cartto, M. Ferrani, G. Martinilli, L. Paglialonga, E. Comin and G. Sberveglieri, *Sens. & Actu. B: Chemical*, **57** (1999) 197.
- [10] M.C. Carotta, M. Ferreni, D. Gnani, V. Guddi, M. Merlim, G. Martinelli, M. Casale and M. Notoro, *Sensors & Actuators*, **B58** (1999) 310.
- [11] R.K. Sharma and M.C. Bhatnagar, *Sensors & Actuators B: Chemical*, **56** (1999) 215.
- [12] S.H. Sai, Y.S. Fung and D.R. Zhu, *Sensors & Actuators B: Chemical*, **108** (2005), 165.
- [13] A. Fujisima, K. Hashimoto and Watamabe, University of Tokyo, BKC, (1999) 46.
- [14] P.R. Mishra and O.N. Srivastava, *Bull. of Mate. Sci.*, **31** (2008) 545.
- [15] H. Homiyara, *Thin Solids Films*, **386** (2001) 173.
- [16] Encyclopedia of Chemical Technology, **24**, 235.
- [17] S.G. Ansari, P. Boroojerdian, S.K. Kulkurni, S.R. Sainkar, R.N. Karekar and R.C. Aiyer, *Journal of Materials Science: Materials in Electronics*, **7** (1996) 267.
- [18] Maria Prudenziati and Morten Bruno, *Thick Film Sensors. An Overview*, *Sensors & Actuators*, **10** (1986) 65.
- [19] C.A. Harper, Handbook of Thick film hybrid Microelectronics, McGraw Hill Book Co. New York, **2** (1974) 6.
- [20] Kiran Jain, R.B. Pant, S.T. Lakshmikumar, Effect of Ni Doping on Thick Film SnO₂ Gas Sensor, *Sensors & Actuators, B: Chemical*, **113** (2006) 823.
- [21] K. Ramkumar, Thick Film Deposition and Processing Short Term Course on Thin and Thick Film Hybrid Microelectronics, Bangalore (1986) 12.11.
- [22] A.T. Nimal, Vijay Kumar, A.K. Gupta, Superconducting Transition Edge Bolometer Based On Single Phase BPSCCO2223 Thick Film, *Indian Journal of Pure and Applied Physics*, **42** (2004) 275.
- [23] L.A. Patil, P.A. Wani, S.R. Sainkar, A. Mitra, G.J. Pathak and D.P. Amalnerkar, Studies on "Fritted" Thick Films of Photo conducting CdS, *Mater. Chem. Phys.*, **55** (1998) 79.
- [24] Peter Tsolovivanov, Design, Fabrication and Characterization of thick film Gas Sensors, Ph.D. Thesis, University Roviva I Virgili, (2004).
- [25] R.S. Khadayate, Research Link-34, 9 Dec.-Feb (2007) 12.
- [26] E. San Andres, M.L. Toledano, Prado A. Del., M.A. Navacerrada, I. Martill, G. Gonzalez-Diaz, W. Bohne, J. Rohrich and E. Strub, *J. Vac. Sci. Techno. A*, **23** (2005)1523.
- [27] Devidas Ramrao Patil and Lalchand Avachit Patil, *IEEE Sensors Journal*, **7** (2007) 434.
- [28] Hengzhong Zhang and Jillian F. Banfield, *J. Phys. Chem. B*, **104** (2000) 3481.
- [29] S. Bakardjieva, J. Subrt, V. Stengl, M.J. Diane and M.J. Sayagues, *Applied Catalysis B: Environmental*, **58** (2005) 193.
- [30] R.A. Spurr and Howard. Myers, Quantitative Analysis of Anatase-Rutile Mixtures with an X-Ray Diffractometer, *Anal. Chem.*, **29** (1957) 760.
- [31] D. Mardare and G.I. Rusu, *Journal of Optoelectronics and Advanced Materials*, **3** (2001) 95.
- [32] H. Tank, K. Prasad, R. Sanjines and F. Levy, *Sensor and Actuators B: Chemical*, 26-27 (1995) 71.
- [33] L. Gao, Q. Li, Z. Song and J. Wang, *Sensors and Actuators B: Chemical*, **71** (2000) 179.
- [34] G. Sberveglieri and L.E. Depero, A novel method for preparation of nanosized TiO₂ Thin films, *J. Adv. Mater.*, **8** (1996) 334.

Influence of Firing Temperature on Compositional and Structural Properties of TiO₂ Thick Films

- [35] H. Hadouda, J. Pouzet, E. Bernede and A. Barrcau, *Mat. Chem. Phys.*, **42** (1995) 291.
- [36] B.D. Cullity, *Elements of X-ray Diffraction*, 2nd Edition (Addition Wesley), (1970) 102.
- [37] A. Teleki, *Sensors and Actuators B: Chemical*, **119** (2006) 683.
- [38] T.B. Gosh, Dhabal Sampa and A.K. Datta, *J. of Applied Phy.*, **94** (2003) 4577.
- [39] N. Savage, B. Chwieroth, A. Ginwalla, B.R. Patton, S.A. Akbar and P. Dutta, *Sensors & Actuators, B: Chemical*, **72** (2001) 239.
- [40] T. Bak, J. Nowotny, M.K. Nowotny and L.R. Sheppard, *J. Aust. Ceramic. Soc.*, **43** (2007)49.